Symmetrical four-bar coupler curves, containing three cusps

Γ	Diffusionskoeffizient
δ	Grenzschichtdicke
ε	Dissipation der turbulenten kinetischen Energie
κ	von Karmansche Konstante
ν	kinematische Zähigkeit
ν_t	Wirbelviskosität
ϕ	allgemeine abhängige Variable
ρ	Dichte
$\sigma_k, \sigma_\varepsilon$	turbulente Prandtlzahlen für die Diffusion von k bzw. ε
τ_w	Wandschubspannung
θ	Öffnungswinkel einer Kanalwand
ξ, η, ζ	Koordinaten des quasi-orthogonalen Koordinatensystems
ω	dimensionsloser Wandabstand

Indizes und Sonderzeichen

Bez	Bezugsgröße
E	im Eintrittsquerschnitt
i, j	Indizes, die die Koordinatenrichtungen bezeichnen
m	Mittelwert
max	Maximalwert
N, S, E, W	Nord-, Süd-, Ost-, West
P	zum Punkt *P* gehörend
R	resultierend
ϕ	für die Variable ϕ

Symmetrical four-bar coupler curves, containing three cusps

Evert A. Dijksman*)

Symmetrical coupler curves are easier to analyse than non-symmetrical ones. This is particular true if one desires to find the double points or the cuspidal points of such curves. It appears that symmetrical coupler curves containing three cusps are governed by one parameter only, which happens to be the coupler-angle. The dimensions of the generating four-bar then meet very simple formulas, enabling the designer of these linkages to face other requirements as well; such as the requirement of a straight-stretch in the coupler curve.

1. Introduction

Cuspidal points or cusps are particular double points of the coupler curve for which the span of time passed between the two coinciding positions ofthe coupler point, tends to zero. In other words, we are dealing with two infinitesimally near positions of the coupler plane for which double point and velocity-pole are coinstantaneous.

Cusps therefore, are to be found at the moving polode of the coupler plane. (The moving polode being the locus of the velocity-poles in the coupler plane.)

Non-rational coupler curves may generally have at most three double points. They are to be found at the circumcircle of the fixed triangle $A_0 B_0 C_0$ which is similar to the coupler triangle ABK of the four-bar [1].

Cuspidal points of the coupler curve are to be seen as particular double points having two coinciding and coinstantaneous double-point-tangents, whence the coupler curve cannot have more than three cusps. In case the coupler curve is symmetrical, one of them should join the axis of symmetry [2], whereas the remaining two are each other's image with respect to the symmetry-axis of the curve. Four-bars, meeting Grashof's rule with the consequence that their shortest bar completely revolves with respect to the other bars, generally produce two branches of the curve.

Then, if we have three cusps, it appears that they won't be seen in only one branch, but are divided in such a way, that the cusp at the axis of symmetry emerge at the one branch, and the remaining ones at the other.

A four-bar resembling a total-rocker generates complete coupler curves, falling apart into two branches when the total-rocker turns into a crank-and-rocker, into a double-crank or into a double-rocker with a revolving coupler.

So, the double-points are either, so-called, own double points of a self-intersecting branch, or otherwise intersection-points of two branches. In reality, the latter are of no technical importance; however, mathematically, they do represent real double points of the complete coupler curve.

Somewhat disturbing[1]) is the fact that pure mathematics even lead to real double points not having real double-point tangents [4; 5]. Such double points are called isolated double points. Fig. 1, for instance, shows the case of three isolated double points of a complete curve produced by a crank-and-rocker mechanism for which $\overline{AB} = \overline{BB_0} = \overline{BK}$, representing the symmetry-conditions of the curve. The isolated, but, from the mathematical point of view, still real double-points, are located at the points D_1, D_2 and $D_3 = B_0$ of the circumcircle of the fixed triangle $A_0 B_0 C_0$; the latter being similar to the coupler-triangle ABK.

These isolated double points become non-isolated through the transition-case, by which the double-point-tangents merge into real but coinciding tangents. The isolated double points then turn into cusps. Thus, a cusp represents a transition-case between an isolated and a non-isolated double point.

If, for example, point B_0 is really attainable by the coupler point, B_0 does represent a non-isolated double point. This occurs when

$$|d-a| \leqq e \leqq d+a \tag{1}$$

*) Dr. *Evert A. Dijksman*, Faculty of Mechanical Engineering, Eindhoven University of Technology, The Netherlands

[1]) Disturbing in the sense that they do not join a family of rotation curves, so-named after *G.R. Veldkamp* [3], as do the self-intersection points of unicursal branches as well as the mixed intersectionpoints of separate branches.

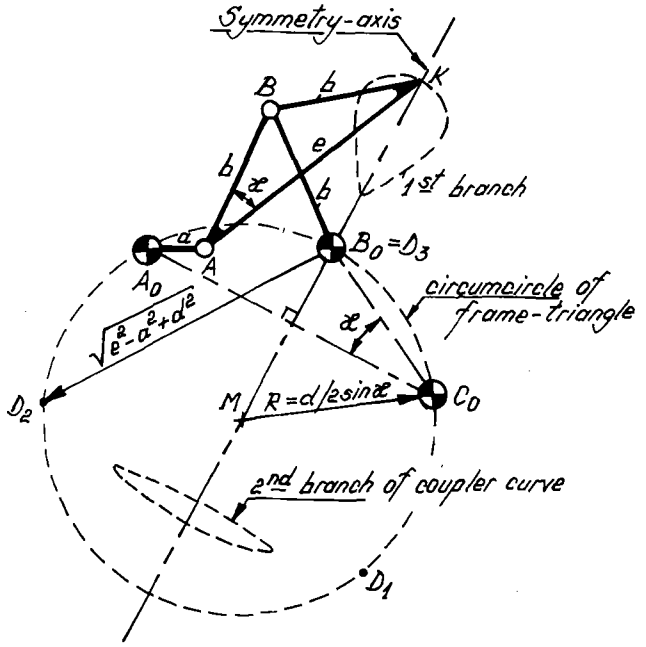

Fig. 1. Three isolated double-points D_1, D_2, D_3 of a bifurcated coupler-curve

If $\sqrt{e^2-a^2+d^2} \leqq 2R = |d/\sin\kappa| \rightarrow D_1, D_2$ are real double points.
If $2b < \sqrt{e^2-a^2+d^2} < 2R \rightarrow D_1, D_2$ are isolated double points

where

$a = \overline{A_0 A}$,

$d = \overline{A_0 B_0}$,

$e = \overline{AK} = 2b \cos\kappa$

and

$\kappa = \sphericalangle BAK$.

Whence, point B_0 turns into a cusp when

$$|d \pm a| = e. \tag{2}$$

The remaining double points, D_1 and D_2 of the curve, are the intersections of the circumcircle about the fixed triangle $A_0 B_0 C_0$ and another circle, about B_0 having a radius equal to the value [2])

$$\sqrt{e^2-a^2+d^2}. \tag{3}$$

It is easily seen that the diameter of the circumcircle equals the value

$$2R = d/\sin\kappa. \tag{4}$$

Thus, D_1 and D_2 are real when

$$\sqrt{e^2-a^2+d^2} \leqq d/\sin|\kappa|. \tag{5}$$

They are real and isolated when

$$2b < \sqrt{e^2-a^2+d^2} \leqq d/\sin|\kappa|. \tag{6}$$

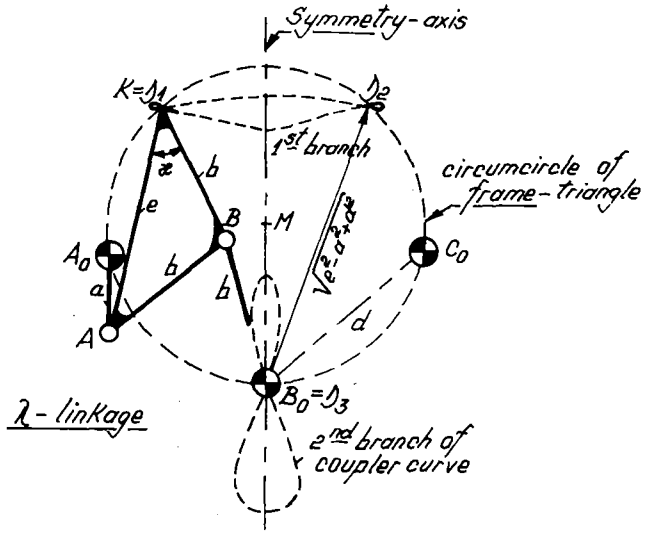

Fig. 2. D_1, D_2 are non-isolated, real double points when $\sqrt{e^2-a^2+d^2} \leqq 2b < |d/\sin\kappa|$

The double points, D_1 and D_2 of the curve, are real and non-isolated when

$$\sqrt{e^2-a^2+d^2} \leqq 2b < d/\sin|\kappa|. \tag{7}$$

In Fig. 2 the three 'own' double points indeed appear in separate branches: D_1 and D_2 for instance, are symmetrically distributed at the first coupler branch, whereas, $D_3 = B_0$, joins the second coupler branch at the common symmetry-axis.

2. Design of the four-bar producing three cusps in her coupler curve

In the 'design-position' of the four-bar for which the coupler-point K coincides with the velocity-pole $P(+B_0)$, the link $A_0 A$ and the 'rocker' $B_0 B$ intersect at $P = K$, Fig. 3.

As further $\overline{A_1 B_1} = \overline{B_1 B_0} = \overline{B_1 K_1}$, the angle $K_1 A_1 B_0 = 90°$. So is

$$\sphericalangle B_0 A_1 A_0 = 90°. \tag{8}$$

Thus, point A_1 meets the circle, joining the points A_0, B_0 and having $\overline{A_0 B_0}$ for diameter.

Point B_0 turns into a cusp of the coupler curve when $K = B_0 = P$ and the bar $A_0 A$ either overlaps the frame, or otherwise lies on the prolonged side of it. This results into the Eq. (2) of the preceding paragraph. For the design-position we then have either $\overline{A_1 K_1} = d - a$ for the first solution, or otherwise $\overline{A_1 K_1'} = d + a$ for the second solution. Indeed the solutions occur in pairs. Further, $\overline{A_0 K_1} = d$ for the first solution, whereas similarly $\overline{A_0 K_1'} = d$ for the second solution. Fig. 3 indeed demonstrates the two solutions.

Anyway, $\sphericalangle A_0 B_0 K_1 = \sphericalangle B_0 K_1 A_0 = \kappa$ which is the coupler-angle of $\Delta A_1 B_1 K_1$. Similarly, $\sphericalangle A_0 B_0 K_1' = \sphericalangle B_1' K_1' A_1 = \kappa'$.

[2]) It is fairly easy to show that the circumcircle of the frame-triangle generally represents a locus for the double-points of the coupler curve [1]. Another locus may be found in the shape of a hyperbola, derived through the coupler curve equation [4; 6]. For symmetrical coupler curves, the hyperbola may degenerate into its asymptotes, leading to four intersection points with the circumcircle, which are the three double points and an initially chosen 4th point. The author obtained the same result in his dissertation [5] based on an expression of *G.T. Bennet* [7], using the isotropic coordinates of *A. Haarbleicher* [8].

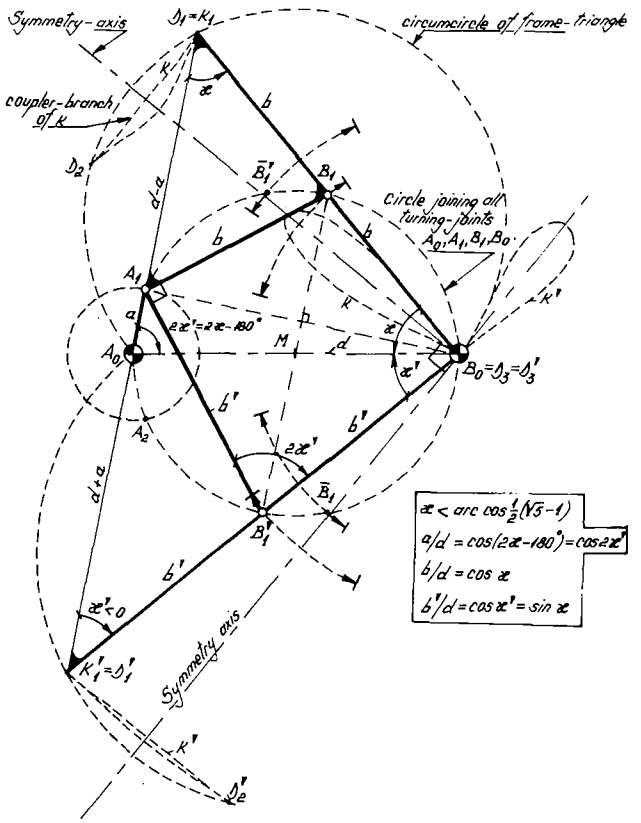

Fig. 3. Two coordinated crank-and-rockers of type λ, each having a common axis of symmetry for their coupler-branches tracing one or two cusps. Each of the bifurcated coupler curves, κ and κ contain three cusps

(Note, that the two perpendicular axes of symmetry also are coinciding double point tangents)

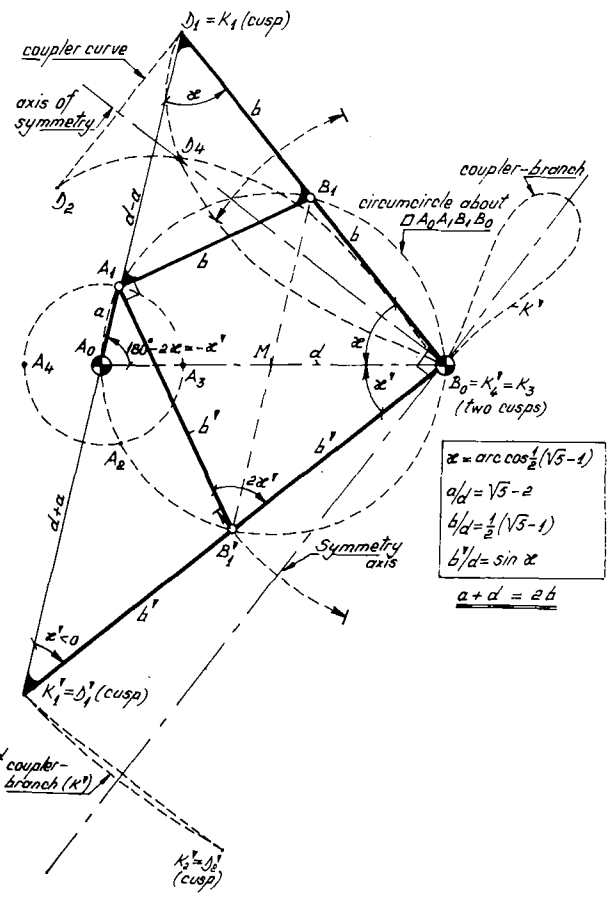

Fig. 4. A folding four-bar and a corresponding crank-and-rocker, each having a coupler curve with three cusps. The folding four-bar with the unicursal couple curve also has a 4th double point D_4 that corresponds to the stretched position of the four-bar. The corresponding crank-and-rocker possesses a bifurcated coupler curve with three cusps distributed over her branches

As $B_1 B_1'$ runs parallel to $K_1 K_1'$, the diagonal $B_1 B_1'$ of the kite-four-bar $A_1 B_1 B_0 B_1'$, joins the center M of the circumcircle about $\Delta A_1 A_0 B_0$. As further $\sphericalangle B_0 B_1 M = \kappa = \sphericalangle A_0 B_0 B_1$, clearly, $\overline{MB_1} = \overline{MB_0} = \overline{MA_0}$.

Hence, B_1 joins the circumcircle about $\Delta A_1 A_0 B_0$. So does the point B_1'.

The isoscales triangle $K_1 A_0 B_0$ reveals that

$$\sphericalangle A_1 A_0 B_0 = 180° - 2\kappa. \tag{9}$$

Similarly, by observing $\Delta A_0 K_1' B_0$, we find that

$$\sphericalangle A_1' A_0 B_0 = -2\kappa' \tag{10}$$

with $A_1' = A_1$.
Thus,

$$\begin{aligned} a/d &= \cos(2\kappa - 180°) = \cos 2\kappa', \\ b/d &= \cos\kappa, \\ b'/d &= \cos\kappa' = \sin\kappa. \end{aligned} \tag{11}$$

In each of the two cases demonstrated, the coupler curve contains two branches, one of them showing a cusp at B_0, whereas the other branch possesses two cusps that are each other's image with respect to the symmetry-axis of the branch.

Clearly, the two solutions are dependent on only one parameter, being the coupler-angle κ. It is therefore possible to change the dimensions by changing the parameter κ. In the particular case, for which $a + d = 2b$, one of the two solu-

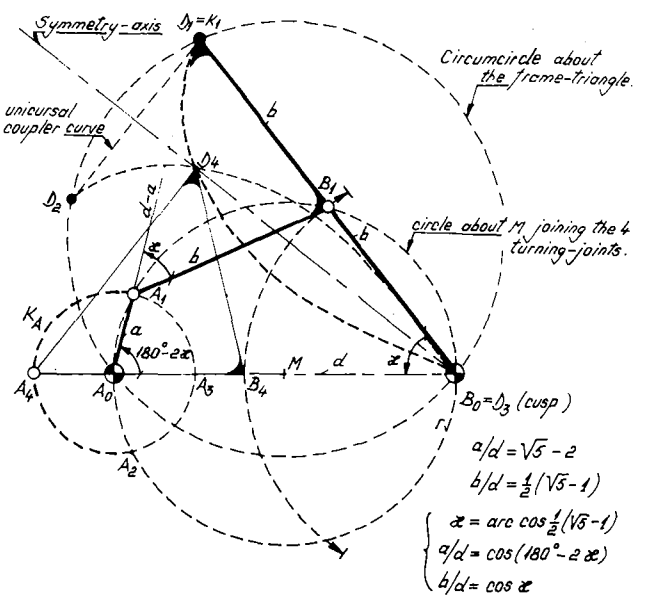

Fig. 5. A folding four-bar producing three cusps and a double-point in her symmetrical coupler-curve

(The cusp at B_0 belongs to the overlapping position, whereas D_4 corresponds to the stretched position $A_4 B_4$)

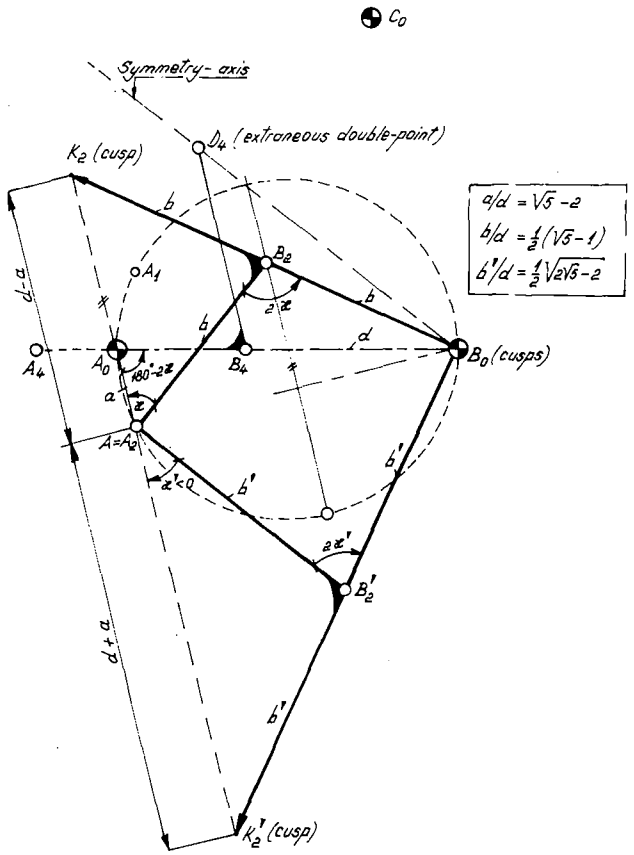

Fig. 6. A folding four-bar, having two symmetrically located cusps, a cusp at B_0, and an extraneous double point at D_4. The corresponding solution resembles a crank-and-rocker, with coupler branches having either one or two cusps. Second position of two interlinked' four-bars, each producing' three cusps in their coupler curves (bifurcated or not)

(Note that B_2 and B_2' do not join the circumcircle about $\Delta A_0 A_2 B_0$)

tions turns into a folding four-bar apparently, for which $\kappa = \arccos \frac{1}{2}(\sqrt{5}-1) = 51{,}8273°$.
Then,

$$a/d = \sqrt{5}-2,$$
$$b/d = \tfrac{1}{2}(\sqrt{5}-1).$$

(See Figs. 4 and 5).

The two branches produced by such a four-bar, then merge into one singular curve, containing three cusps and a fourth double-point joining the axis of symmetry of the then rational coupler curve also being complete and unicursal.

Fig. 6 demonstrates the second position of the combined mechanism of the two solutions by which the two coupler points K and K' attain their two image positions with respect to their symmetry-axes. In this position, the points B_2 and B_2' do not join the circumcircle about $\Delta A_0 A_2 B_0$.

Fig. 7, finally, demonstrates the first, so-called design-position, of the combination, containing a kite-linkage and two *Chebyshev*-dyads that are shunted parallel [9].

The rational coupler curve of the folding four-bar contains a straight-stretch between the cuspidal points D_1 and D_2 of the curve, whence the four-bar may be used as a straight-line mechanism showing zero coupler-point-velocities at the end-positions of the straight-stretch. Clearly, the Figs. 4 and 5 also demonstrate the transition-case, between a crank-and-rocker and a total rocker. If, namely, $\kappa < \arccos \frac{1}{2}(\sqrt{5}-1)$, both solutions are crank-and-rockers.

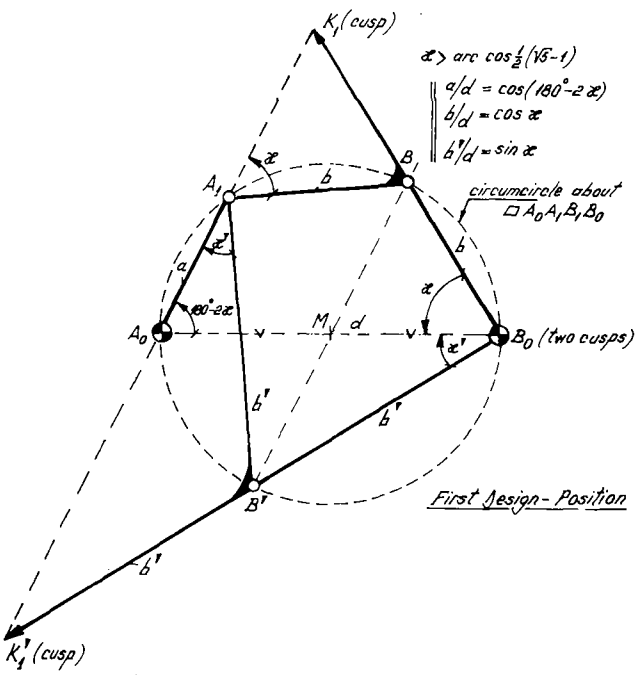

Fig. 7. A total-rocker and a crank-and-rocker as coordinated solutions of λ-type four-bars having three cusps in their respective coupler curves

(Note that the crank $A_0 A$ of the crank-and-rocker needs to be disengaged to produce the complete curve)

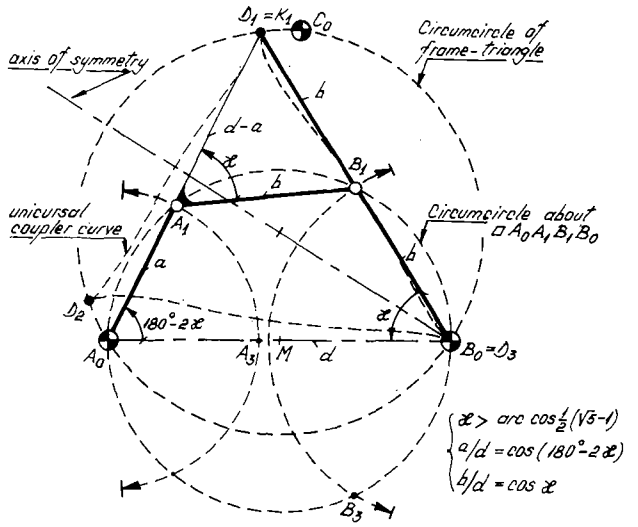

Fig. 8. An internal-internal total-rocker, having three cusps in her unicursal, symmetrical coupler curve

When $\kappa = \arccos \frac{1}{2}(\sqrt{5}-1)$, we embark on a folding four-bar and an additional crank-and-rocker.

If, finally, $\kappa > \arccos \frac{1}{2}(\sqrt{5}-1)$, a total rocker and a crank-and-rocker emerge.

A total rocker containing three cusps in her unicursal and complete coupler curve, demonstrates Fig. 8. The curve approximates a triangle, to be varied by varying the coupler-angle κ.

Conclusion

Only total rockers having internal rocking angles, produce symmetrical, unicursal, but complete four-bar coupler curves,

containing three cusps. They meet very simple equations such as

$a/d = \cos(180° - 2\kappa)$,

$b/d = \cos\kappa$,

$\kappa > \arccos \frac{1}{2}(\sqrt{5}-1)$

being the coupler angle KAB.

In case $\kappa < \arccos \frac{1}{2}(\sqrt{5}-1)$, crank-and-rocker linkages emerge, having either two cusps or otherwise one cusp in their coupler branch. The two branches together, constitute a complete, but bifurcated coupler curve containing three cusps alltogether. For direct applications, see [10; 11; 12].

References

[1] *Beyer, R.:* Kinematische Getriebesynthese. Berlin: Springer Verlag 1953.

[2] *Dijksman, E.A.:* V- und 8-förmige Koppelkurven der Kurbelschwinge. Forschung im Ingenieurwesen 53 (1987) 6, S. 169/184.

[3] *Veldkamp, G.R.:* Rotation Curves. Journal of Mechanisms 2 (1967) 2, p. 147/156.

Note 1: Three cusps in the coupler curve of a random four-bar, not necessarily producing symmetrical coupler curves, are to be obtained in a different way. See, for instance, the general treatment as presented by *Anton Mayer* [14].

Note 2: The theory about coupler curves in general, may be found in VDI-Forschungsheft no. 639 as given by *B. Dizioğlu*. The figures presented in that booklet, are a pleasure to look at, whereas they also represent a survey of all the peculiar possibilities that arise with these four-bar (coupler) curves [15].

[4] *Eckhart, L.:* Konstruktion der Doppelpunkte einer Koppelkurve. Reuleaux Mitt., Archiv für Getriebetechnik, 4 (1936) 12, S. 697/698.

[5] *Dijksman, E.A.:* Synthesis of four-bar linkages with V-shaped, symmetrical coupler curves. Diss. Techn. Univ. Eindhoven 1964.

[6] *Veldkamp, G.R.:* Symmetrische koppelkrommen. DET-Colloquium „Leer der Mechanismen", 13. Febr. 1962, pp. 5/7, T.U. Delft, The Netherlands.

[7] *Bennet, G.T.:* The three bar sectic. Proc. London Math. Soc., 2nd Series, 20 (1920) p. 59/84.

[8] *Haarbleicher, A.:* De l'emploi des droites isotropes comme axes de coördonnées, nouvelle geometrie du triangle. L'Ecôle Polytechnique, Paris (1931).

[9] *Dijksman, E.A.:* Watt-1 Linkages with shunted Chebyshev-dyads, producing symmetrical 6-Bar Curves. MMT. 16 (1981) 2, pp. 153/165.

[10] *Hain, K.:* Koppelkurven mit Spitzen und ihre getriebetechnische Anwendung. Maschinenbau 9 (1941) S. 313/316.

[11] *Hain, K.:* Koppelkurven mit Spitzen an Gelenkvierecken. Feinmechanik und Präzision 49 (1941) 5, S. 61/63.

[12] *Hain, K.:* Angewandte Getriebelehre. Düsseldorf: VDI-Verlag 1961, S. 284/289.

[13] VDI-2728, Blatt 1: Lösung von Bewegungsaufgaben mit symmetrischen Koppelkurven (in Vorbereitung).

[14] *Mayer, A.E.:* Koppelkurven mit drei Spitzen und spezielle Koppelkurven-Büschel. Zeitschrift für Mathematik und Physik 43 (1937) S. 389/445.

[15] *Dizioğlu, B.:* Die Theorie der Koppelkurven. VDI-Forschungsheft 639 (1987).

Received March 13, 1991 F 4072

BÜCHER

Die Schwallströmung von Öl, Wasser und Luft in horizontalen Rohrleitungen. Von *H. Herm Stapelberg* und *D. Mewes*. Inhalt des dieser Zeitschrift angegliederten VDI-Forschungsheftes Bd. 57 (1991) Nr. 668, 60 S., 95 B., 16 Tab., 75 Literaturhinweise, Preis: 109,– DM, für VDI-Mitglieder 98,10 DM.

Die dreiphasige Strömung zweier nichtmischbarer Flüssigkeiten und einer gasförmigen Phase wird in zwei unterschiedlichen horizontalen geraden Rohrleitungen experimentell untersucht. Die Rohre besitzen Durchmesser von 24 bzw. 59 mm und Längen von 10 bzw. 35 m. Als Flüssigkeiten werden Wasser und Öl, als Gas wird Luft eingesetzt. Die Untersuchungen erfolgen bei Drücken bis 3 bar und Umgebungstemperatur. Die maximal einstellbaren Volumenströme betragen 30 m^3/h für die Luft und je 7 m^3/h für die Flüssigkeiten. Die maximale über dem freien Rohrquerschnitt gemittelte Gemischgeschwindigkeit beträgt 3 m/s. Der Anteil der Phase Öl am flüssigen Gemisch wurde zwischen 0 und 100% variiert. In den Experimenten wird der Druckabfall längs der geraden Rohre gemessen und die sich einstellende Strömungsform beobachtet. Der Schwerpunkt der Versuche liegt im Bereich der Schwallströmung. Diese ist gekennzeichnet durch Flüssigkeitspfropfen und große Gaskolben, welche abwechselnd die Rohrleitung durchströmen. Dabei werden zusätzlich die Längen und die Frequenzen der beobachteten Flüssigkeitspfropfen sowie deren Geschwindigkeiten gemessen.

In den Versuchsreihen werden zunächst die Sonderfälle der dreiphasigen Strömung beobachtet: Die zweiphasige Strömung von Öl und Wasser, die von Wasser und Luft sowie die von Öl und Luft. Die beobachteten Strömungsformen für Öl und Wasser werden mit bekannten Forschungsergebnissen verglichen. In einer Strömungsbilderkarte werden die Grenzen der beobachteten Strömungsformen dargestellt. Die gemessenen Reibungsdruckverluste der Strömung zweier nichtmischbarer Flüssigkeiten können mit Hilfe einer neuen Gleichung berechnet werden, ohne die Strömungsformen selbst kennen zu müssen.

Für die Gas-Flüssigkeits-Strömung werden die Grenzen zwischen verschiedenen Strömungsformen ebenfalls experimentell ermittelt. Die Ergebnisse stimmen mit bekannten Strömungsbilderkarten überein. Der Reibungsdruckabfall der dreiphasigen Strömung kann mit Hilfe bekannter für zweiphasige Strömungen gültiger empirischer Berechnungsverfahren ermittelt werden, während die Grenzen der beobachteten Strömungsformen durch eine auf die dreiphasige Strömung erweiterten Strömungsbilderkarte richtig wiedergegeben werden. Der Druckverlust der dreiphasigen Schwallströmung läßt sich ohne die Kenntnis der Strömungsform nicht berechnen. Die Frequenz der Schwallbewegung wird für die dreiphasige Strömung berechnet, indem der Druckverlust der zweiphasigen Strömung von Öl und Wasser sowie die veränderte Schwallbildung für Flüssigkeiten mit höherer Viskosität berücksichtigt werden.

Für kleinere Volumenströme des Gases ist der Schwall nahezu unbegast. In diesem Bereich kann der Druckabfall mit hoher Genauigkeit berechnet werden. Für größere Gasvolumenströme gelingt dies, wenn gemessene Schwallängen oder eine Näherungsgleichung hierfür verwendet werden.

F 668 *D. Mewes*